

Electronic and optical properties of GIZO thin film grown on SiO₂/Si substrates[†]

Dahlang Tahir,^a Eun Kyoung Lee,^b Hyuk Lan Kwon,^b Suhk Kun Oh,^b Hee Jae Kang,^{b*} Sung Heo,^c Eun Ha Lee,^c Jae Gwan Chung,^c Jae Cheol Lee^c and Sven Tougaard^d

The electronic and optical properties of GaInZnO (GIZO) thin films grown on SiO₂/Si by r.f. magnetron sputtering were obtained by means of XPS and reflection electron energy loss spectroscopy (REELS). The optical properties represented by the dielectric function ϵ , refractive index n , extinction coefficient k and transmission coefficient T of GIZO thin films were obtained from a quantitative analysis of the REELS spectra. When the concentration ratios of Ga:In:Zn in GIZO thin films are 1:1:1, 2:2:1, 3:2:1 and 4:2:1, the bandgap values are 3.2, 3.2, 3.4 and 3.6 eV, respectively. The optical properties were determined from the energy loss of the REELS spectra by using quantitative analysis of electron energy loss spectra (QUEELS)- $\epsilon(k, \omega)$ -REELS software. The optical properties depend on the Ga concentration, and the transmission in the visible region improved with increasing Ga concentration in GIZO. Copyright © 2010 John Wiley & Sons, Ltd.

Keywords: REELS; GIZO; bandgap; XPS

Introduction

GaInZnO (abbreviated as GIZO) thin films are promising channel materials for thin-film transistors (TFTs) because GIZO TFTs exhibit large field-effect mobility ($>10 \text{ cm}^2/\text{V s}$) irrespective of their fabrication on various substrates such as silicon, glass, plastic, polyimide, polyethylene terephthalate (PET), cellulose paper and flexible substrates.^[1–5] In addition, they have superior uniformity, low processing temperature, possibility of large-area deposition and long-term stability, and, moreover, they are cost effective.^[4,5]

Kang *et al.*^[6] obtained the optical bandgap and the refractive index for GIZO while varying the compositions of Ga and Zn by using spectroscopic ellipsometry. They showed that the optical bandgap was strongly correlated to the electrical performance of GIZO thin-film transistors, i.e. the turn-on voltage of the drain–source current *versus* gate voltage increased with the increase of the optical gap energy as the Ga/In ratio increased. In recent years,^[1–6] large progress has been made in high-performance TFTs based on GIZO as channel layers. However, the fundamental material properties of GIZO, such as the effect of cation composition on electronic and optical properties, have not been investigated in detail so far. The electronic and optical properties of GIZO thin films are very important in the investigation of transport and electrical properties of TFT devices based on GIZO thin films.

In this paper, we have investigated the electronic and optical properties of GIZO thin films by using reflection electron energy loss spectroscopy (REELS) and X-ray photoelectron spectroscopy (XPS). REELS analysis provides a more straightforward way to obtain the bandgap of any thin film. Quantitative analysis of REELS using the Tougaard algorithm^[7,8] gives us direct information on the optical properties of GIZO thin films through the dielectric function.

Experimental

GIZO thin films were deposited by r.f. magnetron sputtering on SiO₂/Si substrates with the r.f. power of 200 W at room temperature in an argon gas ambient with 1% oxygen added. The composition ratios of Ga:In:Zn in GIZO thin films were 1:1:1 (GIZO1), 2:2:1 (GIZO2), 3:2:1 (GIZO3) and 4:2:1 (GIZO4), which were estimated by using the inductively coupled plasma (ICP) method.^[9] The composition ratios were also confirmed with a quantitative analysis of XPS spectra (Table 1). The physical thickness of deposition for all compositions was 70 nm. To obtain the electronic and optical properties of GIZO thin films, XPS and REELS experiments were carried out by using a VG ESCALAB 210 instrument. XPS spectra were measured using an Al source and at the analyzer pass energy of 20 eV. The incident and take-off angles of electrons for both REELS and XPS were 55° and 0° from the surface normal, respectively. XPS binding energies were referenced to the C 1s peak of carbon contamination at 285 eV. REELS spectra were measured with the primary electron energy of 0.5, 1.0, 1.5 and 1.8 keV for excitation and with the constant

* Correspondence to: Hee Jae Kang, Department of Physics, Chungbuk National University, Cheongju 361-763, Korea. E-mail: hjkang@cnu.ac.kr

† Paper published as part of the ECASIA 2009 special issue.

a Department of Physics, Hasanuddin University, Makassar 90245, Indonesia

b Department of Physics, Chungbuk National University, Cheongju 361-763, Korea

c Analytical Engineering Center, Samsung Advanced Institute of Technology, Suwon 440-600, Korea

d Department of Physics and Chemistry, University of Southern Denmark, DK-5230 Odense, M, Denmark

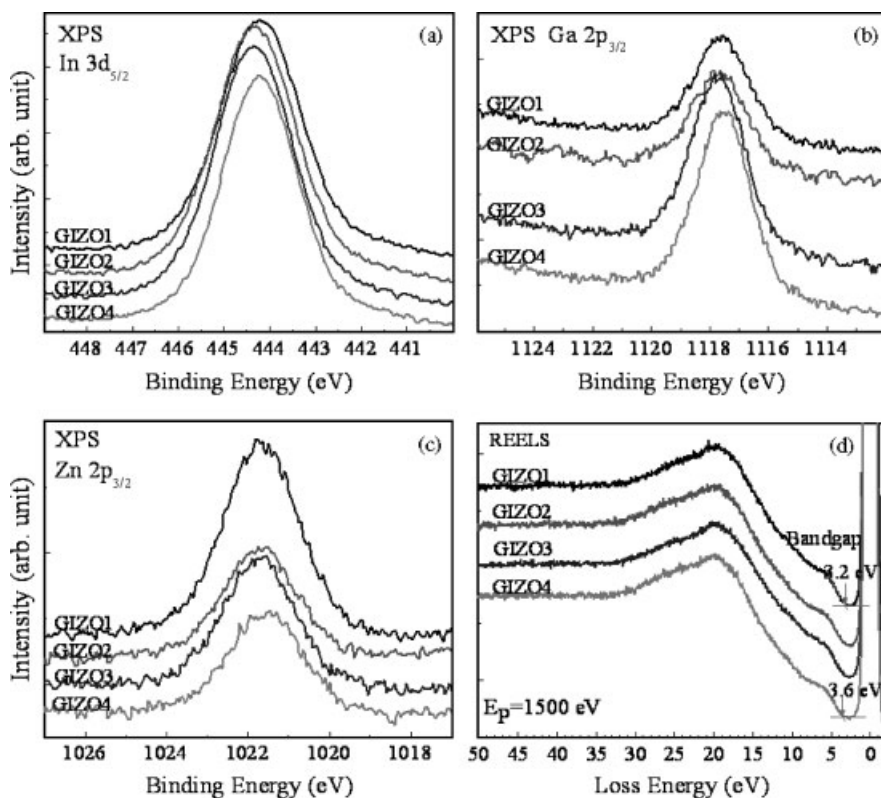


Figure 1. XPS core level photoelectron spectra of (a) In $3d_{5/2}$, (b) Ga $2p_{3/2}$, (c) Zn $2p_{3/2}$ and (d) REELS spectra of GIZO for primary energy of 1500 eV.

analyzer pass energy of 20 eV. The full width at half-maximum (FWHM) of the elastic peak was 0.8 eV.

Results and Discussion

Figure 1(a) shows the In $3d_{5/2}$ XPS peak. The binding energies of the In $3d_{5/2}$ peak were 444.2 eV for GIZO1 and GIZO4 and 444.3 eV for GIZO2 and GIZO3. Within the energy resolution of the XPS system, which is 0.6 eV, the chemical state of the core level In $3d_{5/2}$ does not depend on Ga composition. Figure 1(b) shows the Ga $2p_{3/2}$ XPS peaks. The binding energy for all compositions is 1117.6 eV, which corresponds to the binding energy of the Ga_2O_3 phase. The intensity of the Ga $2p_{3/2}$ peak increases with increasing amount of Ga in GIZO thin films. Figure 1(c) shows Zn $2p_{3/2}$ XPS spectra, which are at 1021.6 eV for all compositions, which corresponds to the binding energy of the ZnO phase. As we see in Fig. 1(c), the intensity of Zn $2p_{3/2}$ peaks decreases with increasing amount of Ga in GIZO thin films. These XPS results therefore show that GIZO thin films have the In_2O_3 , Ga_2O_3 and ZnO phases, independent of the Ga composition. We also obtained the composition ratios of Ga:In:Zn by mean of a quantitative analysis of the XPS spectra as shown in Table 1, which are almost the same as those provided by the ICP method.

We made use of the REELS measurement to find the bandgap values. Figure 1(d) shows the REELS spectra for GIZO thin films. The bandgap values were determined from the energy loss spectrum. The method has been described in our previous article.^[10] The bandgap values for GIZO1, GIZO2, GIZO3 and GIZO4 are 3.2, 3.2, 3.4 and 3.6 eV, respectively. The bandgap values for GIZO1, GIZO2, GIZO3 and GIZO4 obtained by using spectroscopic ellipsometry are 3.17, 3.14, 3.22 and 3.36 eV, respectively.^[6] The bandgap values

Table 1. The composition ratios of Ga:In:Zn in GIZO thin films by the quantitative analysis of XPS spectra

Sample	Ga (%)	In (%)	Zn (%)	O (%)	Ga/In
GIZO1 (1:1:1)	11.8	12.8	11.5	63.8	0.92
GIZO2 (2:2:1)	13.8	14.4	7.3	64.6	0.95
GIZO3 (3:2:1)	18.7	12.2	7.3	61.9	1.53
GIZO4 (4:2:1)	20.9	11.3	6.4	61.3	1.85

for GIZO1 and GIZO2 are almost same, but for GIZO3 and GIZO4 the value is about 0.2 eV smaller than that obtained by using REELS. The compositions for GIZO1, GIZO2, GIZO3 and GIZO4 obtained from XPS quantifications are given in Table 1. As can be seen from Table 1, the bandgap depends on the ratio of Ga to In in GIZO thin films. Both results are found to be increasing with increasing Ga contents with fixed In contents. This phenomenon can be explained in terms of the increase of the Ga_2O_3 phase with increasing Ga content because the bandgap of Ga_2O_3 is about 4.9 eV,^[11] which is larger than that of In_2O_3 (around 3.6 eV for a direct transition and 3.0 eV for an indirect transition)^[12] and ZnO (around 3.37 eV).^[13]

The optical properties of GIZO thin films were determined by a quantitative analysis of the REELS spectra using the Tougaard–Yubero quantitative analysis of electron energy loss spectra (QUEELS)- $\epsilon(k,\omega)$ -REELS software package.^[7,14] The experimental inelastic scattering cross section was found from the measured REELS spectra by utilizing the QUASES-XS-REELS software, which is based on the algorithm in Ref. [15]. Comparison of the theoretical inelastic cross section to experimental inelas-

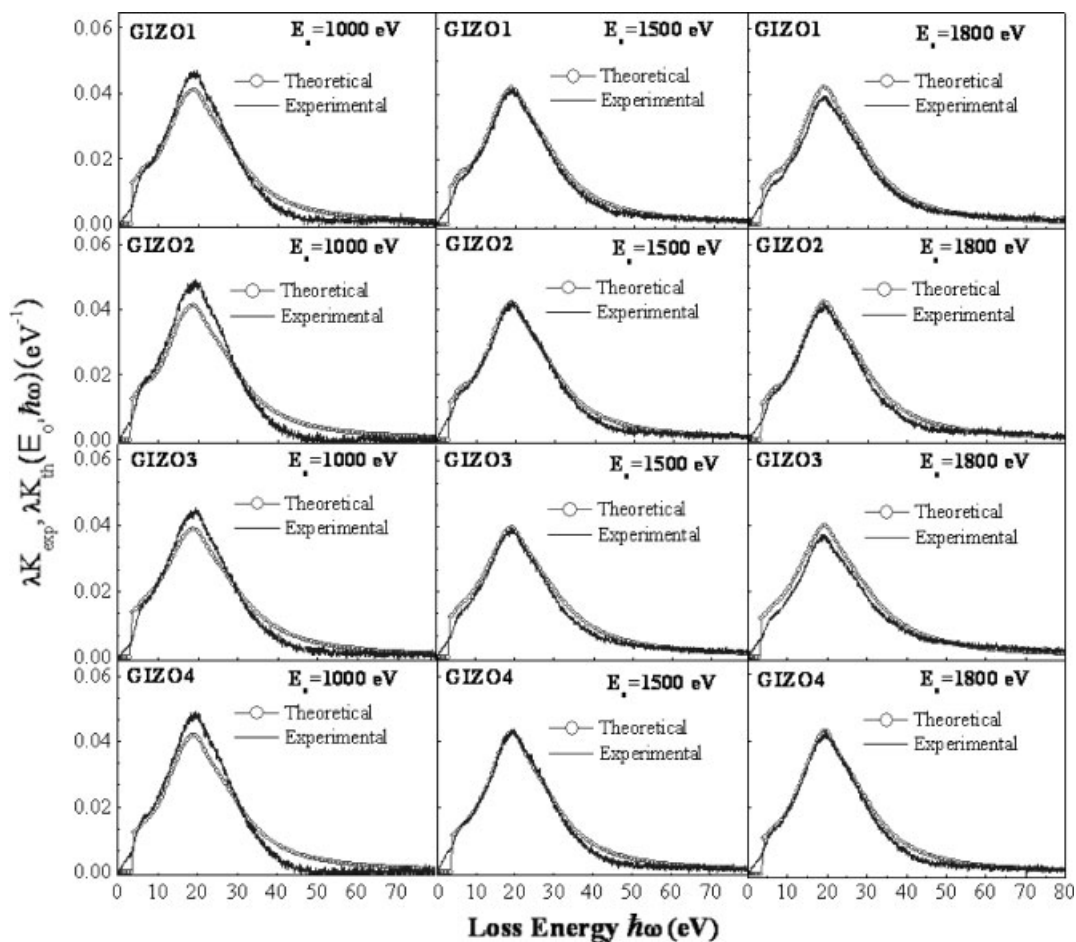


Figure 2. Experimental inelastic cross section λK_{exp} obtained from REELS data (line) compared with the best fit result for the inelastic cross section λK_{th} (symbol) evaluated using the simulated ELF.

tic scattering cross section allows us to determine the dielectric function of the GIZO thin films. The theoretical inelastic scattering cross section was calculated from the dielectric response theory. Assuming that the inelastic process follows a Poisson distribution, the single inelastic scattering cross section $K_{\text{th}}(E_0, \hbar\omega)$ can be evaluated from the inelastic scattering cross section averaged over all possible paths traveled by an electron that has been inelastically scattered only once. Here, E_0 is the primary electron energy and $\hbar\omega$ is the energy lost by an electron in a scattering event. In this model, the response of the material to a moving electron is described by the dielectric function ϵ , which is conveniently described by the energy loss function (ELF) $\text{Im}(-1/\epsilon)$. To evaluate the ELF, we parameterized it as a sum of Drude–Lindhard type oscillators, which is given by Refs [7, 8 and 14–16]:

$$\text{Im} \left\{ \frac{-1}{\epsilon(k, \omega)} \right\} = \theta(\hbar\omega - E_g) \cdot \sum_{i=1}^n \frac{A_i \gamma_i \hbar\omega}{(\hbar^2 \omega_{0ik}^2 - \hbar^2 \omega^2)^2 + \gamma_i^2 \hbar^2 \omega^2} \quad (1)$$

with the dispersion relation $\hbar\omega_{0ik} = \hbar\omega_{0i} + \alpha_i (\hbar^2 k^2 / 2m)$. Here, A_i , γ_i , $\hbar\omega_{0i}$ and α_i are the oscillator strength, damping coefficient, excitation energy and momentum dispersion coefficient of the i th oscillator, respectively. The step function $\theta(\hbar\omega - E_g)$ is included to simulate a possible energy gap E_g , which was estimated from the onset of the energy loss in the REELS spectrum as shown in Fig.1(d). The experimental inelastic cross

sections after background subtraction were fitted with the fitting parameters A_i , γ_i , ω_{0i} and α_i , until good agreement with the calculated inelastic cross section at several primary electron energies was attained. In the calculation, the oscillator strengths A_i in the ELF $\text{Im}(-1/\epsilon)$ was adjusted to make sure that it fulfilled the well-established Kramers–Kronig sum rule^[7,8,14],

$$\frac{2}{\pi} \int_0^{\infty} \text{Im} \left\{ \frac{1}{\epsilon(\hbar\omega)} \right\} \frac{d(\hbar\omega)}{\hbar\omega} = 1 - \frac{1}{n^2} \quad (2)$$

Here n is the index of refraction in the static limit. For GIZO thin film, we note that $1/n^2 \ll 1$.

The theoretical inelastic cross section times the corresponding inelastic mean free path, λK_{th} , is obtained by using QUEELS- $\epsilon(k, \omega)$ -REELS software.^[7,8,17] The inelastic mean free path (λ) was obtained with the inverse of the theoretical inelastic cross section defined in the form:^[7,17]

$$\lambda(E_0) = \left[\int_0^{\infty} K_{\text{th}}(E_0, \hbar\omega) d\hbar\omega \right]^{-1} \quad (3)$$

The value of λ was about 6.6 to 23.3 Å for the primary energy of 500 and 1800 eV, respectively, which are similar for all compositions. Figure 2 shows the experimental λK_{exp} from

the REELS spectra, which is compared with the theoretical λK_{th} resulting from the oscillator parameters of the ELF. These parameters in the ELF were determined via a trial-and-error procedure, until a satisfactory quantitative agreement was reached. Note that, in all the calculations, the same ELF was used for all energies in each composition of GIZO. The agreement between the theoretical results and experimental results is quite good for all energies for each material, and hence the experimentally observed variation in energy is well described by the theory. The ELFs for GIZO thin films were obtained from the REELS spectra for the primary electron energies of 0.5, 1.0, 1.5 and 1.8 keV.

The resulting oscillator parameters of the ELF yield the theoretical λK_{th} that is in good agreement with the experimental λK_{exp} for all energies studied. The obtained parameters for the ELF of GIZO thin film, listed in Table 2, are plotted in Fig. 3(a) for a wide energy range (0–80 eV). The values of the momentum dispersion coefficient α_i are related to the effective mass, e.g. $\alpha_i \approx 0$ for insulators and $\alpha_i \approx 1$ for metals.^[7,8] In accordance with this, we found that good fits were obtained with $\alpha_i = 0.02$ for all oscillators. Figure 3(a) shows the energy loss function (ELF, $\text{Im}\{-1/\varepsilon\}$) and the surface energy loss function (SELF, $\text{Im}\{-1/(1+\varepsilon)\}$). The ELF for GIZO1 has three oscillators in the vicinity of 7, 19.4 and 26 eV, which is similar for all other composition described in this study. The main differences are that the second oscillator for GIZO1 and GIZO2 are the same at 19.4 eV and are shifted to a higher energy loss position for GIZO3 and GIZO4 at 19.6 eV. The widths of this oscillator are 8, 7.6, 7.3 and 7 eV for GIZO1, GIZO2, GIZO3 and GIZO4, respectively. The strength of the oscillator at 7 eV was the same for GIZO1 and GIZO2 and decreases by 0.7 eV for GIZO3 and GIZO4 thin film.

The loss function $\text{Im}\{-1/\varepsilon\}$ allows us to perform a Kramers–Kronig transformation to obtain the real part $\text{Re}\{1/\varepsilon\}$ of the reciprocal of complex dielectric functions. Then we can obtain the real part ε_1 and imaginary part ε_2 by using $\text{Im}\{-1/\varepsilon\}$ and $\text{Re}\{1/\varepsilon\}$, respectively. The real and imaginary parts of the dielectric function

Table 2. Parameters in the model ELFs of GIZO thin film that give the best fit overall to the experimental cross sections at 0.5, 1.0, 1.5 and 1.8 keV

	<i>i</i>	$\hbar\omega_{0i}$ (eV)	A_i (eV ²)	γ_i (eV)
GIZO1	1	7	1.3	4.5
Bandgap 3.2 eV	2	19.4	102.8	8
$\alpha = 0.02$	3	26	370.5	19
GIZO2	1	7	1.3	4.5
Bandgap 3.2 eV	2	19.4	102.3	7.6
$\alpha = 0.02$	3	26	368.8	19
GIZO3	1	7	0.6	5
Bandgap 3.4 eV	2	19.6	78	7.3
$\alpha = 0.02$	3	26	431.1	22
GIZO4	1	7	0.6	5
Bandgap 3.6 eV	2	19.6	94.6	7
$\alpha = 0.02$	3	26	390.5	19

are as follows:^[7,8,14]

$$\varepsilon_1 = \frac{\text{Re}\{1/\varepsilon\}}{(\text{Re}\{1/\varepsilon\})^2 + (\text{Im}\{1/\varepsilon\})^2}, \varepsilon_2 = \frac{\text{Im}\{1/\varepsilon\}}{(\text{Re}\{1/\varepsilon\})^2 + (\text{Im}\{1/\varepsilon\})^2} \quad (4)$$

Figure 3(b) shows the real part ε_1 and imaginary part ε_2 (corresponding to the absorption spectrum) of the dielectric functions. The main peak of ε_1 for GIZO1, GIZO2 and GIZO3 are at around 5.1 eV, and it is shifted to 5.7 eV for GIZO4. The main peaks of ε_2 for GIZO1, GIZO2 and GIZO3 are at around 6.7 eV and is shifted to 7.3 eV for GIZO4 thin film, as can be seen in the inset of Fig. 3(b). The dielectric function for GIZO4 with the largest amount of Ga was thus different from those with a smaller amount of Ga in the GIZO composition.

The refractive index n and the extinction coefficient k in Fig. 3(c) are obtained from dielectric function using the relations^[16]

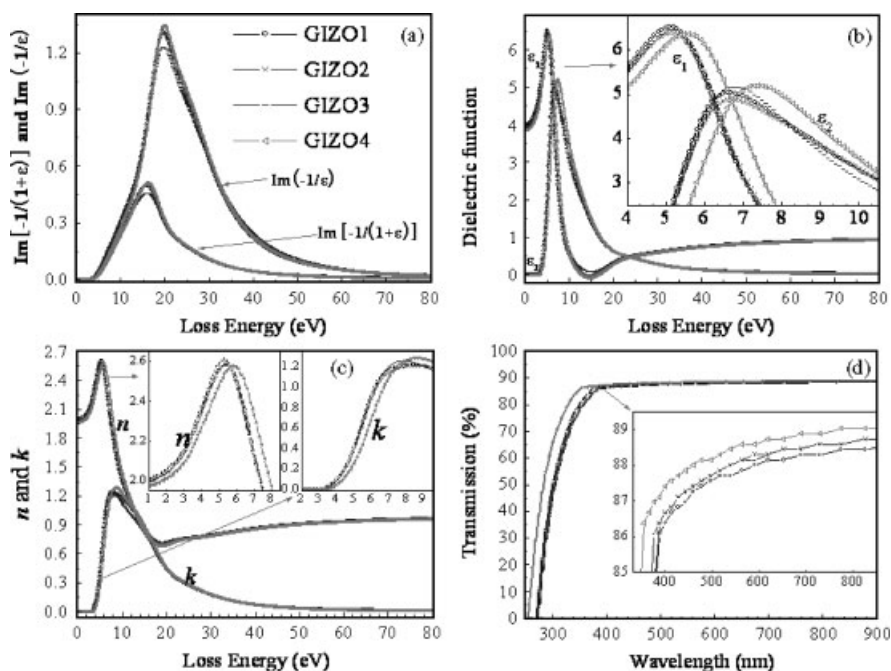


Figure 3. Quantitative REELS spectra of GIZO thin films: (a) ELF and SELF, (b) real part (ε_1) and imaginary part (ε_2) of the dielectric function, (c) refractive indices (n) and extinction coefficient (k) and (d) transmission coefficient as a function of wavelength.

$$n = \sqrt{1/2 \left(\sqrt{\varepsilon_1^2 + \varepsilon_2^2 + \varepsilon_1} \right)} \text{ and } k = \sqrt{1/2 \left(\sqrt{\varepsilon_1^2 + \varepsilon_2^2 - \varepsilon_1} \right)}.$$

As can be seen in the inset of Fig. 3(c), the refractive indices and extinction coefficient function for GIZO4 are different from those of the other GIZO compounds.

We can determine the transmission coefficient T , which is deduced from the relation^[16] $R + T + \mu = 1$. Here R is the reflection coefficient obtained from the refractive index and the extinction coefficient by using the relation $R = [(n - 1)^2 + k^2] / [(n + 1)^2 + k^2]$, and μ is the absorption coefficient related to the extinction coefficient k through, $\mu = 0.82 \times \hbar\omega \times k$, where $\hbar\omega$ is the loss energy. Figure 3(d) shows the optical transmission spectra as a function of wavelength for different amounts of Ga. The transmission coefficient increases in the visible spectral region with increasing amounts of Ga, as can be seen clearly in the inset of Fig. 3(d). These results are comparable to the transmission coefficient of GIZO reported by another group who deposited it at room temperature using pulsed-laser deposition.^[18] It indicates that the optical properties of GIZO thin films do not seriously depend on the amounts of Ga, but the transmission coefficient is enhanced with large amounts of Ga (GIZO4) in the GIZO compound.

Conclusion

We investigated the electronic and optical properties of GIZO thin films with various amounts of Ga in GIZO compounds via REELS and XPS analysis. The bandgap increases from 3.2 to 3.6 eV with increasing amounts of Ga in the GIZO thin films. The optical transmission in the visible region was improved with increasing amounts of Ga in the GIZO thin films. In summary, the quantitative analysis of REELS provides us with a straightforward way to determine the electronic and optical properties of transparent thin-film materials.

Acknowledgement

This work was supported by the Korea Research Foundation Grant funded by the Korean Government (MOEHRD, Basic Research Promotion Fund) (KRF-2008-313-C00225).

References

- [1] W. Lim, E. A. Douglas, S. H. Kim, D. P. Norton, S. J. Pearton, F. Ren, H. Shen, W. H. Chang, *Appl. Phys. Lett.* **2009**, *94*, 072103.
- [2] Y. K. Moon, S. Lee, J. W. Park, D. H. Kim, J. H. Lee, C. O. Jeong, *J. Korean Phys. Soc.* **2009**, *54*, 121.
- [3] J. S. Park, J. K. Jeong, Y. G. Mo, H. D. Kim, S. I. Kim, *Appl. Phys. Lett.* **2007**, *90*, 262106.
- [4] T. Kamiya, K. Nomura, M. Hirano, H. Hosono, *Phys. Status Solidi C* **2008**, *5*, 3098.
- [5] A. J. Leenheer, J. D. Perkins, M. F. A. M. van Hest, J. J. Berry, R. P. O'Hayre, D. S. Ginley, *Phys. Rev. B* **2008**, *77*, 115215.
- [6] D. Kang, L. Song, C. Kim, Y. Park, T. D. Kang, H. S. Lee, Jw. Park, S. H. Choi, H. Lee, *Appl. Phys. Lett.* **2007**, *91*, 091910.
- [7] S. Tougaard, F. Yubero, *QUEELS- $\varepsilon(k, \omega)$ -REELS: Software Package for Quantitative Analysis of Electron Energy Loss Spectra; Dielectric Function Determined by Reflection Electron Energy Loss Spectroscopy, Version 3.0*, **2008**, See <http://www.quases.com>.
- [8] S. Hajati, O. Romanyuk, J. Zemek, S. Tougaard, *Phys. Rev. B* **2008**, *77*, 155403.
- [9] A. Montaser, D. W. Golightly, *Inductively Coupled Plasma in Analytical Atomic Spectroscopy*, Wiley-VCH: New York, **1992**.
- [10] D. Tahir, E. K. Lee, T. T. Tham, S. K. Oh, H. J. Kang, J. Hua, S. Heo, J. C. Park, J. G. Chung, J. C. Lee, *Appl. Phys. Lett.* **2009**, *94*, 212902.
- [11] E. Nogales, B. Sanchez, B. Mendez, J. Piqueras, *Superlattices Microstruct.* **2009**, *45*, 156.
- [12] F. Fuchs, F. Bechstedt, *Phys. Rev. B* **2008**, *77*, 155107.
- [13] M. N. Huda, Y. Yan, S. H. Wei, M. M. Al-Jassim, *Phys. Rev. B* **2008**, *78*, 195204.
- [14] S. Tougaard, F. Yubero, *Surf. Interface Anal.* **2004**, *36*, 824.
- [15] S. Tougaard, I. Chorkendorff, *Phys. Rev. B* **1987**, *35*, 6570. Information on the QUASES-XS_REELS software can be found at www.quases.com.
- [16] F. Wooten, *Optical Properties of Solid*, Academic Press: New York, **1972**.
- [17] D. Tahir, E. K. Lee, S. K. Oh, H. J. Kang, S. Heo, J. G. Chung, J. C. Lee, S. Tougaard, *J. Appl. Phys.* **2009**, *106*, 084108.
- [18] A. Suresh, P. Wellenius, A. Dhawan, J. Muth, *Appl. Phys. Lett.* **2007**, *90*, 123512.